2011 American Control Conference
on O'Farrell Street, San Francisco, CA, USA
June 29 - July 01, 2011

Mode Changing Stability of Wind Turbine in an Integrated Wind Turbine and Rechargeable Battery System

Christine A. Mecklenborg, Dushyant Palejiya, John F. Hall, and Dongmei Chen, Member, IEEE

Abstract— **Power generated by wind turbines changes due to variation in wind speed that is independent of the load power. Rechargeable batteries could be used as a reserve power source to alleviate unbalance between the load power and power generated by wind turbines. A supervisory controller is proposed for an integrated wind turbine–battery system (wind turbine electrically connected to a rechargeable battery). The switching conditions for wind turbine controller operating in multi-input and single-input control modes are discussed. Stability of the wind turbine controller switching between the two modes is analyzed using linearized, open-loop approximation of wind turbine dynamics at the switching instants. A Common Quadratic Lyapunov Function (CQLF) is established for both control modes to prove the system stability. Simulation results demonstrating system stability are also discussed.**

I. INTRODUCTION

Wind is a clean and renewable energy source that is important to the nation's energy security and environmentally sustainability [1], [2]. However, wind energy harvesting in the United States has been low and accounts for only 2.4% of the total electricity supply [3], [4]. A major factor preventing wind energy from becoming a larger contributor is wind power intermittency and its impact on the power grid [1], [5]. The electricity generation from the wind and the consumption from the load must remain balanced to maintain the grid stability. Current approaches to address the wind power intermittency are through wind farm site selection and capacity reserve [6], [7], [8]. Wind farms are selected where the wind source is most stable so that the load demand can be easily followed. There are many forms of capacity reserve, including spin reserve, pumped hydroelectric storage, and compressed air storage [9], [10], [11].The spin reserve is commonly in the form of fossil fuel power plants, and thus has an adverse impact on environment [1], [8]. Both pumped hydro and compressed air methods are limited by the availability of sites and suitable geology [1]. A super grid concept was proposed to achieve the overall grid balance by moving bulk electricity from one place to another over great distances. However, the enormous capital investment and the complexity of system level control renders such a system less feasible [12], [13], [14].

A rechargeable battery has been considered one of the most promising capacity reserve technologies for wind energy due to its zero emission operation and geographical independence. Based on a Department of Energy (DOE) analysis, a total storage capacity of 5 GWh is required to boost the total wind energy contribution to 20% of the nation's overall energy portfolio [1]. This is achievable with advanced Li-ion or a relatively low cost dry cell battery technology. The key is to maximize the wind energy capture while still maintaining the health of the batteries.

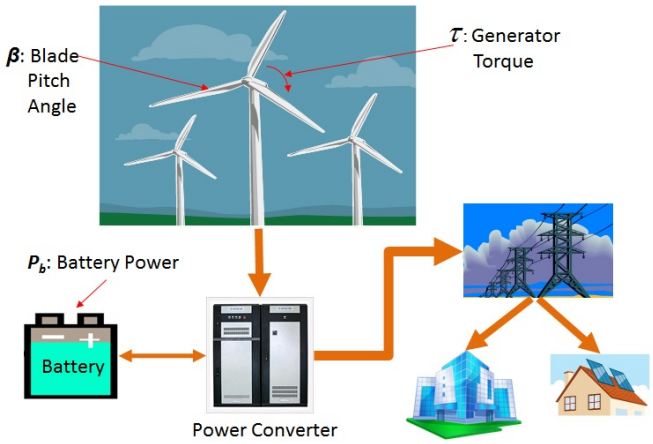

Fig. 1: Integrated wind turbine and battery system

Integrated wind turbine and rechargeable battery system as shown in Fig. 1 present significant challenges for control design. Most existing wind turbine systems do not have a battery storage component. Since meeting load demand is the top priority, existing wind turbines are designed to operate in high wind speed regions, where the available wind power normally exceeds the load demand. Excessive wind power is allowed to pass through without being captured. In an integrated wind turbine and battery system, the amount of wind power captured can be maximized by storing the extra energy in the battery. In order to do so, both the blade pitch angle β of the rotor and the generator torque τ need to be controlled, since the maximum power capture by a wind turbine is a nonlinear function of both τ and β [15]. The battery operation adds additional constraints to the system. To prevent rapid battery aging, the charging and discharging power has to follow certain characteristic profiles after the battery state of charge (SOC) reaches certain limits (e.g., 60% for charging and 20% for discharging) [16]. Falling below the SOC limit in discharging can be avoided by battery sizing in the design stage. In charging, however, the wind turbine output has to be regulated by adjusting the blade pitch angle β, similar to the case of load following. Overall, the control of an integrated wind turbine and battery system switches between two modes as shown in Fig.2 : a MISO (Multi Input Multi Output) mode where the control objective is to maximize the wind power capture by controlling both β and τ, and a SISO (Single Input Single Output) mode where

978-1-4577-0079-8/11/$26.00 ©2011 AACC

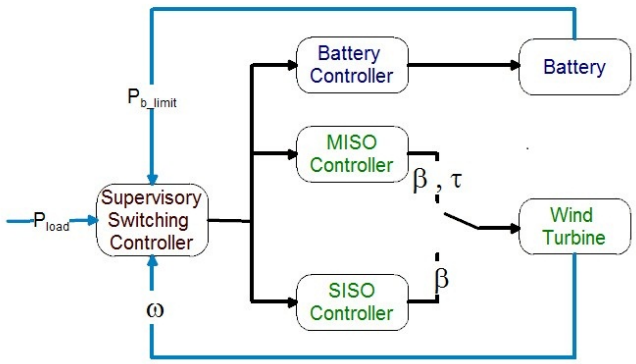

Fig. 2: Control block diagram of Integrated wind turbine and battery system

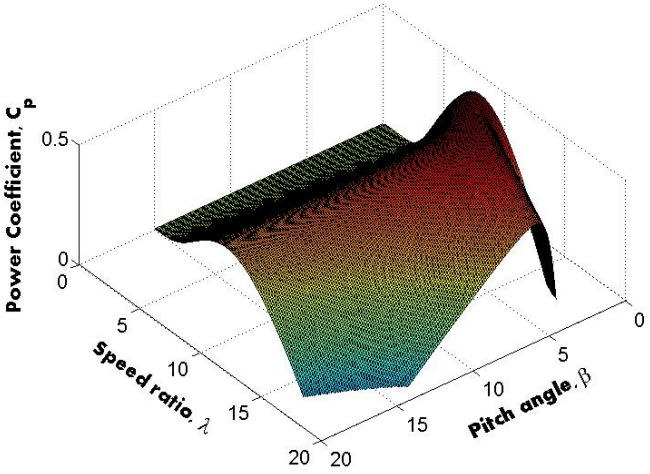

Fig. 3: Wind turbine power coefficient

the objective is to avoid rapid battery aging by regulating only β.

Theoretically, a switched (or hybrid) system is a dynamical system described using a mixture of continuous/discrete dynamic and logic based switching. An example of the switching between MISO and SISO modes can be found in wireless communication applications, where the communication channels are reused to reduce energy consumption [17]. The communication protocol switches between sending multiple signals to one antenna and sending one signal to the same antenna. For this application, the inputs are separated and not necessarily linked by any relationship. The two inputs and the one output of the integrated wind and battery system, on the other hand, are linked. Therefore the control designs for these two types of systems would be different.

The integrated wind turbine and battery system is a new engineering application. The dwell time between different operation modes affects the overall system efficiency for wind energy harvesting. Prior to exploring control design for dwell time estimation, an essential first step is to achieve the system stability during switching. This research focuses on the stability analysis of switching between MISO and the SISO modes. In Section II, we discuss dynamic modeling of the integrated system in MISO and SISO modes. Switching stability of linearized wind turbine dynamics is analyzed in Section III. Section IV describes simulation results and finally, the paper is concluded in Section V.

II. MODELING OF THE INTEGRATED WIND TURBINE AND BATTERY SYSTEM

The dynamic representation of the wind turbine in a switched system has been investigated by authors in [18], [19]. The dynamic model of the integrated system can be represented as [18], [19]

$$\dot{\omega} = \frac{1}{J}\left(\frac{\pi}{8} D_r^2 \rho_{air} C_p \frac{v_w^3}{\omega} - \tau G_r\right) \tag{1}$$

where D_r is the turbine rotor diameter, ρ_{air} is the density of air, v_w is the input wind speed, ω is the turbine rotor speed, J is the combined rotational inertia of the rotor, gearbox, generator, and shafts, G_r is the gearbox gear ratio defined as the generator shaft speed over the rotor shaft speed, τ is the generator torque and C_p is the power coefficient that measures how effectively the wind energy is being converted to mechanical energy. It is a non-linear function of the blade pitch angle β and the tip speed ratio λ

$$C_p = f(\lambda, \beta) \tag{2}$$

The tip speed ratio can be expressed as

$$\lambda = \frac{\omega D_r}{2V_w} \tag{3}$$

Depending on the values of β and λ, the power coefficient C_p slides on the surface shown in Fig. 3. This surface is constructed based on available wind turbine data and a CFD model [20]. The first term on the right-hand side of (1) determines the wind power that can be captured. The second term is the power at the generator end.

Figure 2 shows the control block diagram of an integrated wind turbine rechargeable battery system. The primary objective of the system is to satisfy the load demand P_{load} with combination of wind turbine and battery power and thus reducing variations in wind power. Meeting this objective means battery needs to be recharged from time to time. There are three inputs to the system: 1) P_{load} is the load requirement 2) v_w is the wind speed and 3) $P_{\text{b\_limit}}$ is the charging - discharging power threshold for rechargeable battery. Blade pitch angle β and generator torque τ are the control inputs to control power generated by the wind turbine. Depending on values of the wind speed v_w, load power P_{load} and status of available battery power, the system operates in one of the two control modes:

1) *MISO:* when the available wind power is not sufficient to meet P_{load} and $P_{\text{b\_limit}}$, both τ and β are used to control the turbine speed in order to reach the maximum C_p, thus achieving the maximum power. This is MISO mode.

2) *SISO:* when the turbine can generate more power than P_{load} and $P_{\text{b\_limit}}$, the generator power is limited to the sum of P_{load} and $P_{\text{b\_limit}}$

$$\tau\omega G_r = P_{load} + P_{\text{b\_limit}} \tag{4}$$

which yields

$$\tau = \frac{P_{load} + P_{\text{b\_limit}}}{\omega G_r} \tag{5}$$

By substituting (5) into (1), we have

$$\dot{\omega} = \frac{1}{J}\left(\frac{\pi}{8} D_r^2 \rho_{air} C_p \frac{v_w^3}{\omega} - \frac{P_{load} + P_{\text{b\_limit}}}{\omega}\right) \tag{6}$$

Equation (1) indicates that the pitch angle β alone is sufficient to control turbine speed in order to achieve the load following. The system switches between the MISO and SISO modes represented by (1) and (6) according to switching conditions based on the available wind power, load demand and status of available battery power. Even though the wind turbine could be represented by a straightforward linear model after much simplification, the switching control design is much more complicated. This is a common characteristic shared by many switched systems [21], [22].

A common approach to wind turbine control is to partition the turbine operation into two main regions according to the wind speed [23]. In low speed region, the control objective is to maximize wind energy capture while in high speed region the objective is to limit the captured wind power up to a safe electrical and mechanical load limit. The switching between these two regions depends solely on the input wind speed. It is also not desirable for the wind turbine to switch back to low speed region because without another power source the wind turbine along will not meet the load demand. Therefore, the switching between regions does not happen often. However, for an integrated wind turbine–battery system described above, the switching between control modes occurs more frequently and it depends not only on the wind speed but also on the load power and the battery's charge status.

III. WIND TURBINE CONTROLLER STABILITY

In this section, we analyze the stability of the wind turbine dynamics that switches between MISO and SISO controllers. One of the well known and standard methods in switching system stability analysis is the use of converse theorems to find common quadratic Lyapunov function (CQLF) [21]. In order to use the converse Lyapunov theorems, the integrated system needs to be linearized; local linearization of the wind turbine system will provide a good approximation of the dynamic system within a small region.

The wind turbine dynamics in MISO mode (1) can be linearized around a switching point $\omega_0, \beta_0, \tau_0, v_{w0}$ as follows: Equation (1), more generally, can be written as

$$\dot{\omega} = f(\omega, \beta, \tau) \tag{7}$$

to emphasis ω is a system variable and β, τ are control inputs. Linearizing (7), we have

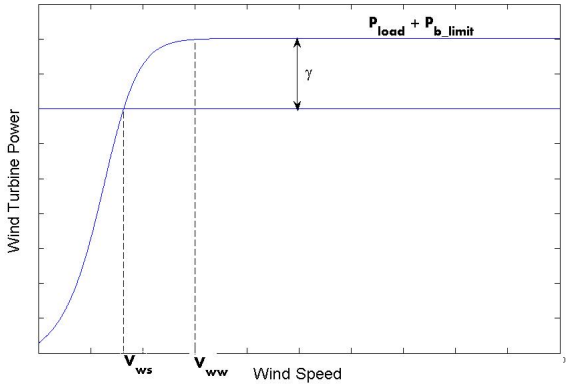

Fig. 4: Switching with strong and weak CQLF

$$\begin{aligned}\dot{\omega} =& f(\omega_0, \beta_0, \tau_0) + \left.\frac{\partial f(\omega, \beta, \tau)}{\partial \omega}\right|_s (\omega - \omega_0) \\ &+ \left.\frac{\partial f(\omega, \beta, \tau)}{\partial \beta}\right|_s (\beta - \beta_0) + \left.\frac{\partial f(\omega, \beta, \tau)}{\partial \tau}\right|_s (\tau - \tau_0)\end{aligned}$$

Substituting f from (1), the above equation becomes

$$\begin{aligned}\dot{\omega} =& \frac{1}{J}\left(\frac{\pi}{8} D_r^2 \rho_{air} C_{p0} \frac{v_{w0}^3}{\omega_0} - G_r \tau_0\right) \\ &+ \frac{1}{J}\left(\frac{\pi}{8} D_r^2 \rho_{air} C_{p0} v_{w0}^3\right) \frac{-1}{\omega_0^2} (\omega - \omega_0) \\ &+ \frac{1}{J}\left(\frac{\pi}{8} D_r^2 \rho_{air} \frac{v_{w0}^3}{\omega_0}\right) \left.\frac{\partial C_p}{\partial \beta}\right|_s (\beta - \beta_0) - \frac{G_r}{J}(\tau - \tau_0)\end{aligned} \tag{8}$$

Note that the wind power coefficient C_p map is continuous and smooth as shown in Fig. 3. Additionally, wind turbine and battery parameters, such as the C_p and the battery capacity fade, change slower than the switching dynamics and can be considered constant during the switching period. This quasi-steady value of C_p at the switching instant assumes to be C_{p0}. Equation (8) is simplified to

$$\begin{aligned}\dot{\omega} =& \frac{1}{J}\left(\frac{\pi}{8} D_r^2 \rho_{air} C_{p0} \frac{v_{w0}^3}{\omega_0} - G_r \tau_0\right) \\ &+ \frac{1}{J}\left(\frac{\pi}{8} D_r^2 \rho_{air} C_{p0} v_{w0}^3\right) \frac{-1}{\omega_0^2} (\omega - \omega_0) - \frac{G_r}{J}(\tau - \tau_0)\end{aligned} \tag{9}$$

The generator torque τ is a control input and as such it can be set independently of the rotor speed. Here, we focus on open-loop system - system without control inputs - as a first step in stability analysis of the integrated system. Not considering input τ and constant terms, (9) can be written as an open-loop system

$$\dot{\omega} = -\frac{c_1}{\omega_0^2}\omega + 2\frac{c_1}{\omega_0} \tag{10}$$

where c_1 is defined as $c_1 = \frac{1}{J}\left(\frac{\pi}{8} D_r^2 \rho_{air} C_{p0} v_{w0}^3\right)$.

Similarly SISO system in (6) can be linearized at a switching point $\omega = \omega_0$ with the corresponding C_{p0} and v_{w0} as follows:

$$\dot{\omega} = -\frac{1}{\omega_0^2}(c_1 - c_2)\omega \tag{11}$$

where $c_2 = \frac{1}{J}(P_{load} + P_{\text{b\_limit}})$.

Equations (10) and (11) form open-loop, linear and time-invariant approximations of the original system in (1) and (6), allowing us to apply standard techniques of stability analysis.

According to the converse Lyapunov theorems [24], a switched system consisting of two or more linear time invariant (LTI) subsystems defined as

$$\Sigma A_i : \dot{x}(t) = A_i x(t), A_i \in \mathbb{R}^{nxn}, i \in 1,2,\ldots,m$$

is a stable switching system if:

1) All A_i are Hurwitz;
2) There exists CQLF for all LTI subsystems A_i.

The sufficient condition for the existence of a CQLF is that a matrix $P = P^T > 0, P \in \mathbb{R}^{nxn}$ should simultaneously satisfy Lyapunov equations

$$A_i^T P + P A_i = -Q_i, i \in 1,2,\ldots,m \tag{12}$$

If $Q_i > 0, V(x) = x^T P x$ is said to be a strong CQLF but for $Q_i \geq 0, V(x) = x^T P x$ is said to be a weak CQLF [21].

It is obvious to observe that the state transition matrix in (10)

$$A_{MISO} = -\frac{c_1}{\omega_0^2}$$

is Hurwitz because c_1 is positive during wind turbine operation. For linearized system in SISO mode, the state transition matrix in (11) is

$$A_{SISO} = -\frac{1}{\omega_0^2}(c_1 - c_2)$$

The system switches from MISO to SISO mode when wind energy capture is larger than the combined load and battery threshold power. Therefore, at the instant when the system switches to the SISO mode the following inequality holds.

$$\frac{\pi}{8} D_r^2 \rho_{air} C_p v_w^3 \geq P_{load} + P_{\text{b\_limit}} \tag{13}$$

which means $c_1 \geq c_2$, thus making A_{SISO} Hurwitz. By choosing $P = P^T = 1$ and substituting in (12), we have

$$Q_{MISO} = 2\frac{c_1}{\omega_0^2} > 0 \quad \text{and} \quad Q_{SISO} = 2\frac{1}{\omega_0^2}(c_1 - c_2) \geq 0$$

So there exist a weak CQLF,

$$V(\omega) = \omega^T P \omega = \omega^2$$

for the integrated wind turbine with battery system, establishing Lyapunov stability.

At the switching instance, if $c_1 > c_2$, then there will be a strong CQLF implying that the system is asymptotically stable. It is desirable to achieve asymptotic stability in SISO mode so that the system could be robust to errors. In order to ensure asymptotic stability in SISO mode, the following must be satisfied

$$c_1 > c_2 \tag{14}$$

It is clear from (14) that the c_1 needs to be increased and/or c_2 be decreased. Examining the c_1 definition, we realize c_1 cannot be increased as it is proportional to the power from the turbine at a switching instant and the turbine is most likely to be operating at maximum C_p when switching from MISO to SISO mode. Even if the turbine is not operating at maximum C_p, the dependence of c_1 on wind speed and nonlinear, smooth C_p map rules it out from increasing it. On the other hand, c_2 is proportional to the generator power, which can be limited to lower value than the one proposed in Section II. Defining a new term c_2' to represent a reduced value of c_2,

$$c_2' = P_{load} + P_{\text{b\_limit}} - \gamma \tag{15}$$

where $\gamma > 0$. Since the load power cannot be manipulated, decrease in c_2 is achieved by reducing the battery charging threshold $P_{\text{b\_limit}}$ by γ. In practice, this translates into slower battery charging rate.

With the reduced generator power, the switching condition from MISO to SISO in (13) is modified as

$$\frac{\pi}{8} D_r^2 \rho_{air} C_p v_w^3 > P_{load} + P_{\text{b\_limit}} - \gamma \tag{16}$$

Figure 4 shows the power vs. wind speed plot for a typical variable speed turbine with variable pitch control. Wind speed V_{ww} in that figure is the switching wind speed in case of weak CQLF. Lowering the switching power threshold by γ in order to ensure strong CQLF will result in lower switching wind speed V_{ws} as shown in Fig. 4. This is not desirable as generated power will be limited at lower wind speed resulting in lower wind energy capture. However, the difference $\Delta c = c_1 - c_2'$ determines the rate of convergence in SISO system and it is desirable to have a larger Δc for faster convergence in SISO mode, which implies lower switching wind speeds. There is a trade-off between the system stability and the wind energy capture. An optimal point should be defined.

To reflect the lower limit on generator power expressed in (15), the SISO dynamics in (6) is changed to

$$\dot{\omega} = \frac{1}{J}\left(\frac{\pi}{8} D_r^2 \rho_{air} C_p \frac{v_w^3}{\omega} - \frac{P_{load} + P_{\text{b\_limit}} - \gamma}{\omega}\right) \tag{17}$$

and the switching condition from SISO to MISO is modified to

$$\frac{\pi}{8} D_r^2 \rho_{air} C_p v_w^3 < P_{load} + P_{\text{b\_limit}} - \gamma \tag{18}$$

Above stability analysis is for linearized, autonomous system – an ideal situation. Studies will be conducted to include effects of control inputs, nonlinearities, disturbances other than the wind speed, plant uncertainties and the delay of the generator torque actuator when it switches in and out of the control loop.

IV. SIMULATION RESULTS

To validate the stability of the system when it switches between MISO and SISO modes, simulations were performed on a system with following parameters:

- Rated Wind Power = 100 kW
- Rotor Diameter(D_r) = 18.5 m
- Rotor Inertia (J) = 26000 kg m ^{2}
- Maximum Power Coefficient (C_{pmax}) = 0.4412

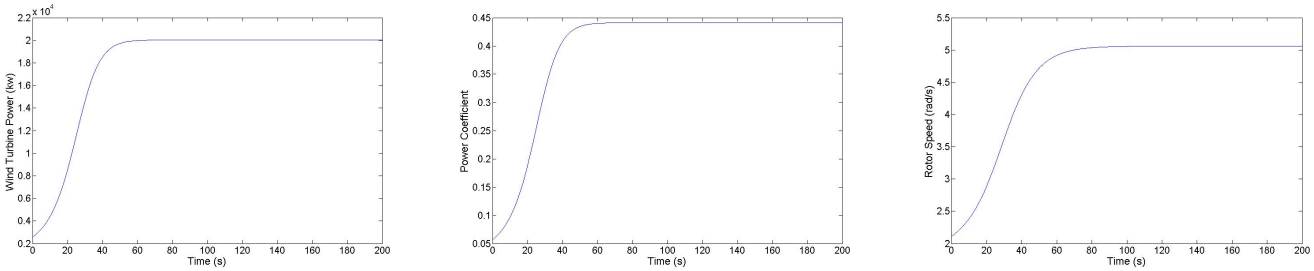

(a) Wind turbine power (b) Power Coefficient (c) Rotor Speed

Fig. 5: Constant wind speed system variables

- Battery charging - discharging power threshold ($P_{\text{b\_limit}}$) = 5 kW
- Load demand (P_{load})= 25 kW

The system is simulated under three different wind speed conditions; In the first case, the wind speed and power demand is held at a constant value. For the second case, the system is simulated with wind speed data based on real wind measurements but the power demand is constant. In order to assess the effects of varying load demand, third simulation was performed with real wind measurements and varying load demand.

A. Constant Wind Speed and Load Demand

We choose 6.5 m/s wind speed as the input to the system so that switching condition in (13) is not true. It will ensure the system starts in the MISO mode and stays in it. The primary objective in the MISO mode is to maximize wind power capture. It is achieved by using control inputs β and τ to drive turbine towards maximum power coefficient C_{pmax} according to controller described in [23]. Figure 5a shows wind turbine power vs. time. Power gradually increases as the system moves toward C_{pmax} as shown in Figure 5b till it reaches maximum of 20 kW. Figure 5c shows that the rotor speed is stabilized at 5 rad/s after the controller has achieved its objective of attaining C_{pmax}.

B. NREL Wind Profile Data and Constant Load Demand

National Renewable Energy Laboratory (NREL) provides datasets of wind speed measurements at 10 minute intervals recorded across the US [25]. For the control design, higher resolution wind speed data is needed. So the power spectral density of an NREL dataset is calculated in order to extract wind speed at a higher resolution in time domain [26]. Figure 6a shows the extracted wind speed, which varies at high frequency, for 200 s. Even though the wind speed varies at high frequency, the turbine responds to slower wind speed variations due to its large inertia.

Figure 6a also shows wind speed after applying a low pass/moving average filter that averages data over 10 s. The system starts in the MISO mode during which the controller drives the system toward C_{pmax} (C_p is shown in Fig. 6c) but before it can reach C_{pmax}, the rapidly increasing power (in Fig. 6b) reaches the limit set by $P_{load} + P_{\text{b\_limit}}$ (30 kW).

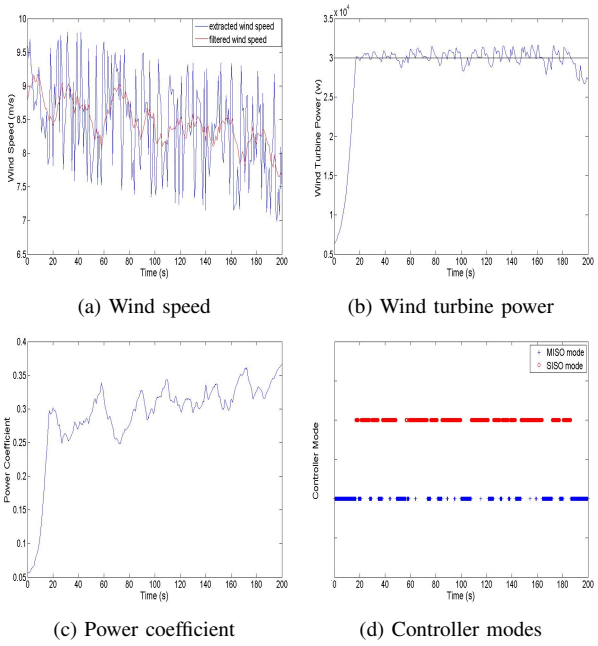

(a) Wind speed (b) Wind turbine power

(c) Power coefficient (d) Controller modes

Fig. 6: Simulation with NREL wind profile data

So the controller switches to SISO mode at 18 s when both power and C_p stop increasing as shown in Fig. 6b and 6c respectively. In this mode the controller objective is to limit power to 30 kW. From this point on, the controller continues to switch between two modes, as shown in Fig. 6d, in response to wind speed variations while meeting control objectives. Due to its large inertia, it is impossible for wind turbine to maintain power at a single value in changing wind, however the power overshoot/undershoot is limited to 2 kW as seen in Fig. 6b. Figure 6c also reveals that C_p is slowly increasing, however intermittently, across stable control mode switches from 18 s to 200 s.

C. NREL Wind Profile Data and Varying Load Demand

This case simulates the effect of varying demand power on switching stability. The demand power is simulated to vary between 25 to 30 kW. It follows the pattern of the daily power requirement in California documented in [27], where the demand gradually rises throughout the day but falls quickly during the night. Figure 7b shows the demand

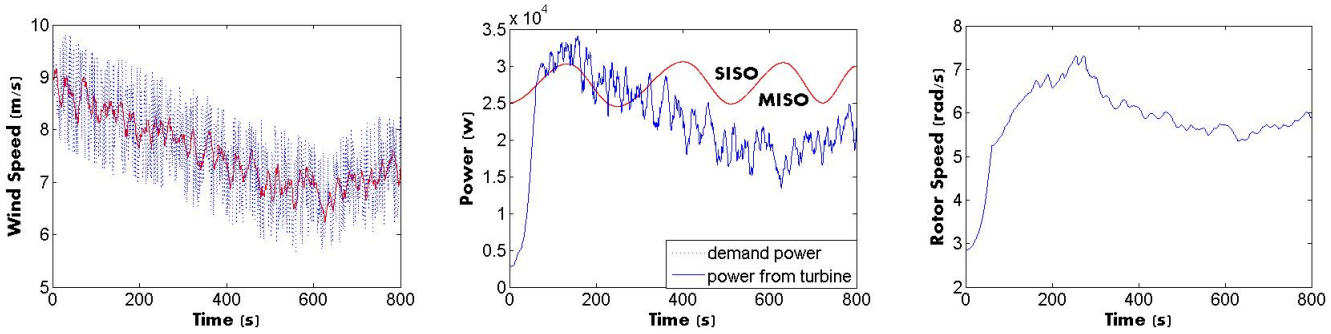

(a) Varying Wind Speed (b) Wind turbine power (c) Rotor Speed

Fig. 7: Varying load demand simulation

power and turbine power. The wind speed input from NREL data is shown in Fig. 7a.

The system starts in the MISO mode during which the controller drives the system toward C_{pmax}. The rapidly increasing power (in Fig. 7b) reaches the limit set by $P_{load} + P_{\text{b\_limit}}$ (30 kW). So the controller switches to SISO mode at 60 s and it starts to track the demand power until 326 s when a low wind speed forces the system to switch to the MISO mode. Similar to case B, it is impossible for a wind turbine to maintain its output power at a single value in a changing wind speed, however the output power to the grid from an integrated system could be more stable due to the ability of battery to absorb/supply any overshoots/undershoots in turbine power.

V. CONCLUSIONS

We have presented a supervisory switching controller for an integrated wind turbine and rechargeable battery system. Switching between wind turbine control modes is determined not only by the wind speed but also by the load demand and the battery's charge status. Switching stability of linearized system has been established using CQLF function. Simulations were performed under varying wind speed conditions to demonstrate the system stability.

REFERENCES

[1] US Department of Energy "Funding Opportunity Announcement, DE-FOA-0000290-GRIDS", 2010.

[2] "Annual Energy Review, Report No. DOE/EIA-0384, United States Department of Energy, Energy Information Administration, 2008.

[3] D. U. E. I. Administration. (2008) [On line]. http://www.eia.doe.gov/cneaf/electricity/epa/epat1p2.html

[4] World Wind Energy Report 2008, World Wind Energy Association, February 2009.

[5] L. Global Energy Concepts, New Mexico Resources Assessment: Lee Ranch Data, Online Abstracts and *Reports of Sandia National Laboratories*, February, 2003.

[6] Vilhauer, M. Y. a. R., "Sri Lanka Wind Farm Analysis and Site Selection Assistance," *National Renewable Energy Laboratory*, NREL/SR-710-34646, August 2003.

[7] Hansen, L.H., Helle, L., Blaabjerg, F., Ritchie, E., Munk-Nielsen, S., Bindner, H., Sorensen, P., and Bak-Jensen, B., Conceptual Survey of Generators and Power Electronics for Wind Turbines, *Report of Riso National Laboratory*, Roskilde, Denmark, December 2001 .

[8] Bose, B.K., Energy, Environment, and Advances in Power Electronics, *IEEE Transactions on Power Electronics*, v. 15, no. 4, July 2000.

[9] Bueno, C. and Carta, J.A., Wind Powered Pumped Hydro Storage Systems, A Means of Increasing The Penetration of Renewable Energy in The Canary Islands, *Renewable and Sustainable Energy Reviews*, v. 10, iss. 4, pp. 312-340, August 2006.

[10] Finley, B., Compressed Air Wind Energy Storage, *Energy Bulletin*, November 27, 2005.

[11] Bullough, C., Gatzen, C., Jakiel, C, Koller, M., Nowi, A., and Zunft, S., Advanced Adiabatic Compressed Air Energy Storage for the Integration of Wind Energy, *Proceedings of the European Wind Energy Conference*, EWEC 2004, November 22-25, 2004, London, UK.

[12] Chu, S., US Energy Secretary, Investing in Our Energy Future,*presentation of Grid Week*, Washington DC, September 21, 2009.

[13] Ibrahim, H., Ilinca, A, and Perron, J., Energy Storage Systems-Characteristics and Comparisons, *Renewable and Sustainable Energy Reviews*, v. 12, iss. 5, pp. 1221-1250, June 2008.

[14] Battaglini, A., Lilliestam, J., Hass, A., and Patt, A., Development of SuperSmart Grids for a More Efficient Utilisation of Electricity from Renewable Sources, *Journal of Cleaner Production*, v. 17, iss. 10, pp. 911-918, July 2009.

[15] Creaby, J., Li, Y., and Se, J.E., Maximizing Wind Turbine Energy Capture using Multivariable Extremum Seeking Control, *Wind Engineering*, vol. 33, no. 4, 2009 pp 361388.

[16] Private conversation with Xtreme Power Inc.

[17] Siam, M.Z. and Krunz, M., Channel Access Scheme for MIMO-Enabled Ad Hoc Networks with Adaptive Diversity/Multiplexing Gains, *Mobile Netw. Appl.* 2009, pp.433-450

[18] Patel, M., "Wind and Solar Power Systems Design, Analysis, and Operation," Taylor & Francis, Boca Raton FL, 2006.

[19] Hau, E., "Wind Turbines: Fundamentals, Technologies, Application, Economics," Springer, Berlin, 2006.

[20] S. Heier, "Grid Integration of Wind Energy Conversion Systems", John Wiley & Sons. Ltd., 1998.

[21] Shorten, R., Wirth, F., Mason, O., Wulff, K., and King, C., Stability Criteria for Switched and Hybrid Systems, *SIAM Review*, Vol. 49, Iss. 4, November 2007, pp. 545-592 .

[22] Liberzon, D., and Morse, A.S., Basic Problems in Stability and Design of Switched Systems, *IEEE Control Systems Magazine*, 1999.

[23] Johnson, K.E., Pao, L.Y., Balas, M.J., and Fingersh, L.J., Control of Variable-Speed Wind Turbines Standard and Adaptive Techniques for Maximizing Energy Capture, *IEEE Control System Magazine*, pp. 70-81, June 2006.

[24] Molchanov, P. and Pyatnitskii, E. S., Criteria of Asymptotic Stability of Differential And Difference Inclusions Encountered in Control Theory, *Systems Control Letters*, vol. 13, 1989, pp. 5964.

[25] NREL Wind Integration Datasets (online), http://www.nrel.gov/wind/integrationdatasets/about.html

[26] Manwell J., 2009, "Wind energy explained : theory, design and application", Wiley, Chichester U.K.

[27] http://www.mpoweruk.com/electricity demand.htm